Development of an Experimental Model of Low Frequency Dipole Radiation in the Presence of Multilayered Structures

M. Shifatul Islam
and Sadman Shafi
Anyeshan Limited
Dhaka-1208, Bangladesh
Email: shifatul@anyeshan.com

Mohammad Ariful Haque
Bangladesh University of
Engineering and Technology
Dhaka-1000, Bangladesh
Email: arifulhoque@eee.buet.ac.bd

***Abstract*—The behaviour of electromagnetic fields in the presence of layered media has been studied and explored a lot, and utilized in numerous applications involving radio wave propagation. However, the works were done on simplified geometrical models, with ideal point dipole approximations, and therefore, were not practically very feasible. In this paper, we have developed a finite element method (FEM) simulation model which can be used to analyze practical dipole radiation characteristics in the low frequency (LF) near-field zone. The simulation environment is developed, and tested for various three-layered systems and compared with the results obtained using existing analytical methods. Both the analytical and the FEM simulation results indicate that the near-field response has strong dependence on the medium dielectric properties and thickness. The electric field vs. radial distance profiles have minima whose corresponding radial distances increase with increasing thickness of the dielectric, but decrease with the increase of the dielectric constant. These results appear to contain significant information on the medium dimensions and dielectric characteristics, signifying LF measurements to be a promising method for non-destructive measurements. Also, a slightly more complex structure with spherical air pores is examined and the field values, which could not be computed analytically, are determined through simulation. This overcomes the primary limitation of the analytical methods where one must always assume uniform layered structures for such calculations, and therefore the exploration domain is generalized.**

I. Introduction

The response of electromagnetic (EM) fields in the presence of a multilayered system has been of a lot of interest in the field of electromagnetic engineering. The problem was first tackled by Sommerfeld [1], who solved the field problem of a dipole above a single semi-infinite halfspace using the Hertz potential approach and formulated the field expressions in the presence of an infinitely long ground. The two layered problem was extended to generalized N layered structures by Wait and Brekhovskikh et al. [2], [3]. In those works, the source and receiver were always in free space. Later in the 70's, Kong et al. [4] first provided the expressions of electromagnetic fields for all dipole configurations in the presence of arbitrarily stratified media, and later other researchers [5], [6] generalized the solution to the complete problem by considering medium anisotropy and arbitrary source receiver locations. Since then, the solution was used to investigate a lot of applications such as far-field propagation, [2], characterization of geophysical substances such as lunar samples and glacier regions [7]–[10] etc. Many of these works were done in the far-field region and the researchers were forced to assume simplified structures due to the complexity of the field solutions. In addition, the stratifications of the media considered in these works were planar. Other types of stratification, such as spherical [11], [12], cylindrical [13] and arbitrary non-planar stratifications [14] have also been investigated.

With the availability of new EM and physics simulation tools, it is possible to examine complex structures while avoiding the pitfalls of the analytical methods. In such an approach, just the relevant experimental environment is designed, and the field responses are computed by the model itself using the finite element method (FEM). FEM methods are becoming increasingly popular, and have been used to examine and theorize different phenomena in photonics, optics, and other VHF (very high frequency) wave-matter interactions [15]–[17]. In contrast, [18] has analytically demonstrated the feasibility of using low frequency EM waves to characterize the properties and dimensions of bulk geophysical substances, like glacier, sea ice or layered grounds. The work also highlighted the theoretical limits, within which the method is applicable. A low frequency FEM model can greatly aid the investigation of such an LF response with a practical dipole configuration. Furthermore, it can be used to explore a wide variety of layered geometries.

In this paper, we have attempted to design a finite element system, which is capable of determining the field values in the near-field zone, and explored several layered structures. The paper is divided into four sections. In section II we present the existing theory and expressions to compute EM fields in the presence of a layered medium. In section III we discuss about the experimental arrangement with different three layered geometries. In section IV, first we describe the methods to evaluate the required field values using analytical treatment. Then we highlight upon our approach for the FEM modelling environment and modelling procedure. In section

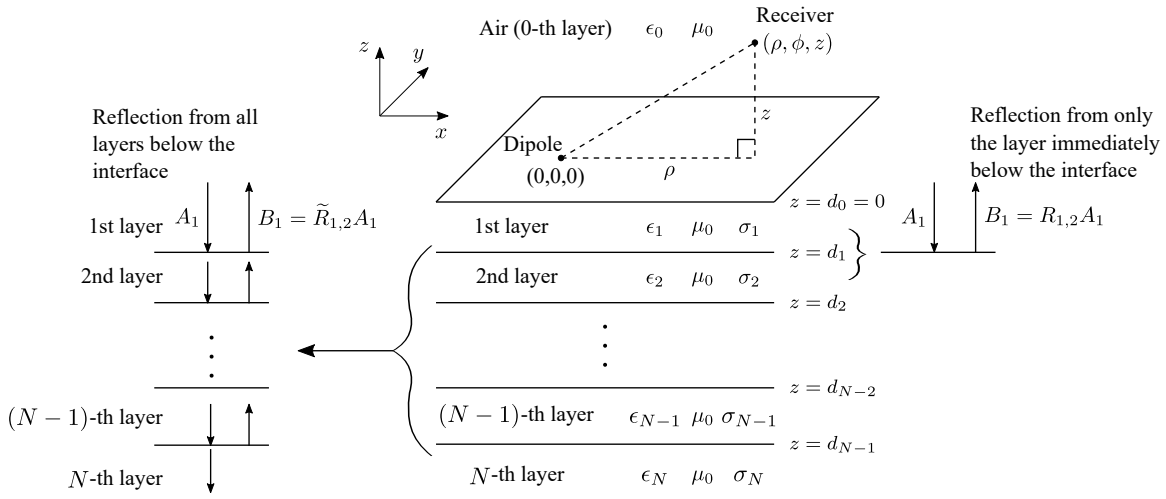

Fig. 1. A schematic arrangement of a horizontal electric dipole located above a multilayered structure.

V, we interpret the field magnitudes with varying substrate dielectric properties and thickness, and also compare the results obtained from analytical and FEM measurements to describe the overall feasibility of the models. Finally, we draw general conclusions in section VI.

II. Dipole above a layered medium

For this work, we will assume a horizontal electric dipole (HED) pointed towards the positive x-axis. The source is placed above an N-layer uniform layered structure. The permittivity, permeability, conductivity and loss tangent of the i-th layer are ϵ_i, μ_i, σ_i and $\tan\delta_i$ respectively. The top layer is the 0-th layer (also called the source medium), which is assumed to be air or vacuum, while the bottom (N-th) layer is semi-infinite. The dielectric constant of the i-th layer is $\epsilon_{ri} = \frac{\epsilon_i}{\epsilon_0}$. We choose a cylindrical coordinate system due to cylindrical symmetry of the layered geometry and write the field expressions using (ρ, ϕ, z) coordinates. A schematic arrangement of the geometry is shown in Fig. 1.

For the expressions of HED above a layered medium, we assume the source has a $e^{-j\omega t}$ dependence with time, where $\omega = 2\pi f$ is the angular frequency of the HED, and f is its frequency. For analyzing the field response in the presence of an inhomogeneous structure we need to determine the planewave reflection coefficients of the system and incorporate them in the Sommerfeld representation of the fields, [1] to get the total field response.

For a horizontal electric dipole configuration, there exist both TE (Transverse Electric) and TM (Transverse Magnetic) polarized waves, and the equations of the reflection coefficients for such polarizations are:

$$\widetilde{R}^{TM}_{m,\ m+1} = \frac{R^{TM}_{m,\ m+1} + \widetilde{R}^{TM}_{m+1,m+2} e^{2ik_{z,m+1}h_{m+1}}}{1 + R^{TM}_{m,\ m+1}\widetilde{R}^{TM}_{m+1,m+2} e^{2ik_{z,m+1}h_{m+1}}} \tag{1}$$

Here, $\widetilde{R}^{TM}_{m,\ m+1}$ is the total reflection coefficient seen from the m-th layer to below and $h_m = |d_m - d_{m-1}|$ is the thickness of the m-th layer. $R^{TM}_{m,m+1}$ denotes the TM reflection coefficient between the m-th and $(m+1)$-th layers only, and is given by:

$$R^{TM}_{m,m+1} = \frac{\left(\epsilon_{m+1} + i\frac{\sigma_{m+1}}{\omega}\right)k_{z,m} - \left(\epsilon_m + i\frac{\sigma_m}{\omega}\right)k_{z,m+1}}{\left(\epsilon_{m+1} + i\frac{\sigma_{m+1}}{\omega}\right)k_{z,m} + \left(\epsilon_m + i\frac{\sigma_m}{\omega}\right)k_{z,m+1}} \tag{2}$$

The reflection coefficients for TE waves have forms similar to (1), except we replace $\widetilde{R}^{TM}_{m,\ m+1}$ and $R^{TM}_{m,m+1}$ with $\widetilde{R}^{TE}_{m,\ m+1}$ and $R^{TE}_{m,m+1}$ respectively. Here,

$$R^{TE}_{m,m+1} = \frac{\mu_{m+1}k_{z,m} - \mu_m k_{z,m+1}}{\mu_{m+1}k_{z,m} + \mu_m k_{z,m+1}} \tag{3}$$

and if we assume nonmagnetic materials ($\mu_m = \mu_{m+1} = \mu_0$), then

$$R^{TE}_{m,m+1} = \frac{k_{z,m} - k_{z,m+1}}{k_{z,m} + k_{z,m+1}}. \tag{4}$$

Instead of dealing with all the TM and TE field components, it is efficient to focus on the longitudinal z-components H_z and E_z only, as they are the only decoupled components. All other TM and TE components can be presented in terms of these two components using Maxwell's equations [4], [19]. The equations for E_z and H_z in the source medium are:

$$E_z = \int_{-\infty}^{\infty} i\frac{Il}{8\pi\omega\epsilon}\left[k_\rho^2\left(1 - \widetilde{R}^{TM}\right)e^{ik_z z}H_1^{(1)}(k_\rho\rho)\cos\phi\right]dk_\rho \tag{5a}$$

$$H_z = \int_{-\infty}^{\infty} i\frac{Il}{8\pi}\left[\frac{k_\rho^2}{k_z}\left(1 + \widetilde{R}^{TE}\right)e^{ik_z z}H_1^{(1)}(k_\rho\rho)\sin\phi\right]dk_\rho \tag{5b}$$

Here, k_ρ, which is a free variable running from $-\infty$ to ∞, is the propagation component along the cylindrical ρ-axis, and $k_{z,i} = \sqrt{k_i^2 - k_\rho^2}$ is the propagation component along the direction of the stratification (z-axis) and k_i is the propagation

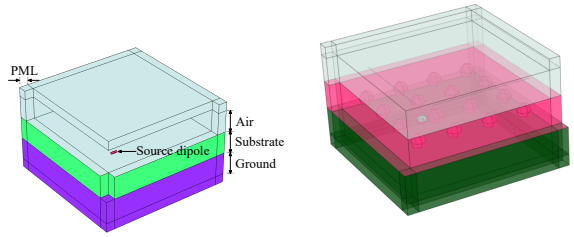

(a) (b)

Fig. 2. Geometrical arrangement of (a) the three layered system and (b) the complex geometry

wavenumber in the i-th layer. For the source medium, we suppress the subscripts and write k and k_z only in (5a) and (5b). Among the other variables, I is the driving current, l is the length of the dipole, ϕ is the angle measured from the positive x-axis (the azimuth angle of the receiver), and $H_\nu^{(1)}(.)$ is the Hankel function of the first kind with order ν.

III. Simulation Setup

For our study of the field behaviour in the LF near-field zone, we have first chosen a simplified three layered system, where the top layer is the lossless source air medium, the middle layer is a material with an arbitrary permittivity (ϵ_1) and a very low dielectric loss ($\tan\delta_1 = \frac{\sigma_1}{\omega} = 0.005$), and the bottom layer is a semi-infinite ground with a very high conductivity ($\tan\delta_2 \to \infty$). For the ease of discussion, we describe the middle layer as the "substrate". Such structures are very well-known and can be observed in various geophysical substances [18], [20], [21]. The operating frequency is 1 MHz, which is also the frequency at which the loss tangents are defined. All three media are assumed to be nonmagnetic ($\mu_0 = \mu_1 = \mu_2$). We perform a radial sweep of the receiver in the LF near-field zone, from 2 m to 20 m from the source in the endfire direction and measure the magnitude of E_z. Among E_z and H_z, H_z depends on the TE reflection coefficient, and the medium dielectric constants are not directly related to the TE reflections. And in [18] it has been shown that the magnitude of H_z does not vary significantly with varying dielectric constants when the loss is too low. So here we focus our attention on $|E_z|$, which is a function of the TM reflection coefficients, which are directly related to the changes of the medium dielectric constants. We examine the field variations for the following cases:

- The dielectric constant of the substrate is varied with $\epsilon_{r1} = 5, 10, 20$ and the fields are observed along the radial line.
- The thickness of the substrate is varied from 1 m to 5 m for each value of dielectric constant and the field variations are noticed.

Finally, we simulate a more complex geometry using the finite element structure, where the second layer is assumed to be consisting of small air pores, which are lumped and modelled as discrete spheres placed at intervals. First, we simulate this system for an operating frequency of 1 MHz to see the effect of the pores in the field profiles, and later, we elevate the frequency to 10 MHz, to observe if the increased frequency causes any significant scattering by the pores.

IV. Methodology

A. Analytical computation of field values

The analytical computation has two parts - the computation of the reflection coefficients of the layered system and then the integral values as a whole. The steps are:

- **Computing the reflection coefficient:** In order to compute the total reflection coefficient at the top surface $\widetilde{R}_{0,1}^{TM}$, we start by exploiting the fact that the bottom layer is infinite and therefore $\widetilde{R}_{N-1,\ N}^{TM} = R_{N-1,\ N}^{TM}$. Then we use (1) recursively from the bottom up all the way to the top surface, and determine $\widetilde{R}_{0,1}^{TM}$. The same process applies for determining $\widetilde{R}_{0,1}^{TE}$.
- **Computing the Sommerfeld integrals:** The Sommerfeld integrals are of the form:

$$\int_{-\infty}^{\infty} f(k_\rho) e^{ig(k_\rho)} H_1(k_\rho \rho) dk_\rho \tag{6}$$

which is similar to (5a). The integral is in general a complex integral with multiple poles and branch points [19] with oscillatory nature of the Hankel function. Although the straightforward computation is not simple and robust, there exist several methods to compute them. Among them, the modified Simpson's rule [18], [19], [22], [23], DFT method [18], [21], Romberg's method [24], and the recent Gauss-Kronrod [25] and Legendre quadratures [26], [27] are noteworthy. We have used the modified Simpson's integration method for computation, which has been found to be computationally very efficient in the LF near-field zone.

B. Finite Element Modelling and Simulation

Finite element simulations are useful in determining EM fields given they are comparatively simpler to implement. Computational complications associated with the analytical methods can be avoided if finite element models are used. Furthermore, they can be used to investigate the response of the EM fields for complex structures. If we wish to measure fields along both broadside and endfire directions, we need to use 3D geometries, where modelling is not straightforward. For 3D simulations, there are two computational limits that prevent these simulations to be arbitrarily precise.

- The mesh elements cannot be arbitrarily fine to provide the perfect solution at each point, since the finer the mesh elements are, the more the computational memory requirement is.
- A relatively coarse mesh will result in error propagation through the element nodes and the results at distant points from the source will give erroneous values [28].

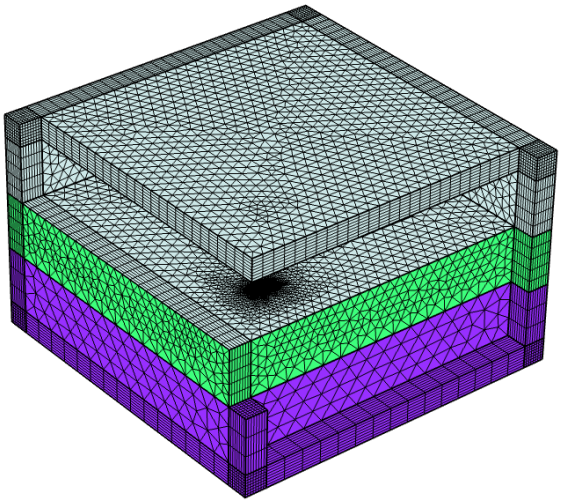

Fig. 3. A convenient view of the meshing arrangement

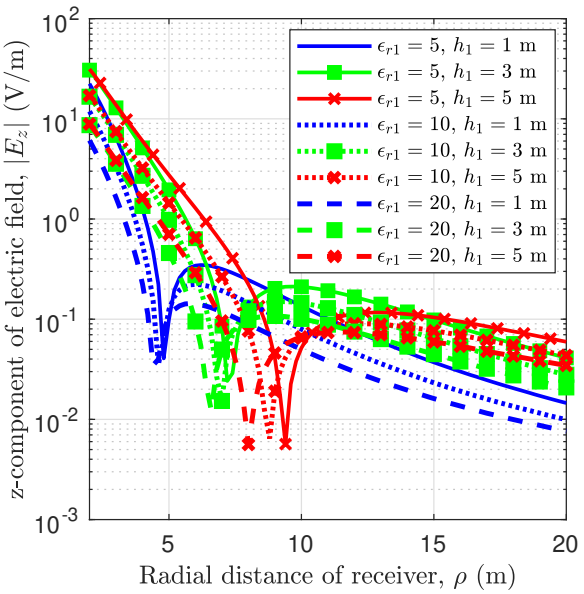

Fig. 4. Variation of $|E_z|$ with change of thickness and dielectric properties of the substrate, obtained using analytical methods.

A balance has to be struck while considering these two constraints and the boundary conditions need to be appropriately defined to model the simulation environment properly.

For FEM simulation, we use COMSOL Multiphysics, and use the electromagnetic waves physics in the frequency domain. To set up the desired experimental arrangement, which is a radial sweep of magnitude from 2 m to 20 m, we have taken the following steps to implement the FEM system to practically model the "dipole-above-layered-medium" system.

- **Designing Geometry:** Our defined geometry has dimensions 30 m×30 m, slightly higher than required for the radial sweep. This is to maintain a distance between the source and the boundaries of the geometrical domain. Keeping the source neighborhood sufficiently distant from the nearest boundary minimizes the effect of boundary reflection near the source, which is critical. The geometry is shown in Fig. 2.
- **Setting up Boundary:** For properly defining the boundary, we have used the PML (Perfectly matched layer) approximation for the external boundaries of the domain. We have found good results for a PML thickness of 2 m, and when the PML is modelled using swept mesh with more than 4 distributed layers. For low performance computations, an alternative is to use scattering boundary conditions (SBC) but generally they are inferior to PML in terms of resolution.
- **Modelling the Dipoles:** For simulation, we modelled both an ideal dipole and a real short dipole to contrast the results with those of the analytical method and model a practical scenario. The ideal dipole is assumed to be a point, excited by an ideal current source along the x-axis, while the real dipole is formed by connecting two short cylindrical wires with a lumped port, since the dimensions are way lower than the operating wavelength.
- **Mesh Construction:** The optimization of the mesh was critical to address the performance with the given memory specification. For this purpose, source neighborhood is meshed with a very high concentration. For the ideal dipole, we define a small sphere surrounding the source point and put high mesh concentration in that spherical domain, while for the real dipole, the cylindrical wires are given a high concentration. The source neighborhood domain of interest (air-substrate vicinity) is given slightly coarse mesh, and the remaining geometry mesh was relatively course. Careful meshing near the source ensured minimum error near the source, which in turn reduced error propagation outside. The swept mesh is used to model the PML, and for 8 elements across a section, the result appeared to converge well. A convenient view of the meshing is shown in Fig. 3.

V. Results and Discussions

In this section we present the results obtained through analytical computation and FEM simulations as described in the previous section and examine if the dielectric constant and dimensional variations can be noticed. First, the analytical results are presented in Fig. 4.

From the figure we can immediately observe that the $|E_z|$ profiles have noticeable local minima. The locations of the minima are dependent on the thickness of the substrate in the following way:

- With the increase of the substrate thickness, for a given dielectric constant, the radial distance of the minimum position increases. After the minimum location is crossed, the magnitude rises and then falls, and this decrease is greater for a lower thickness. This phenomenon in the LF near-field zone is explained in [18], and the presence

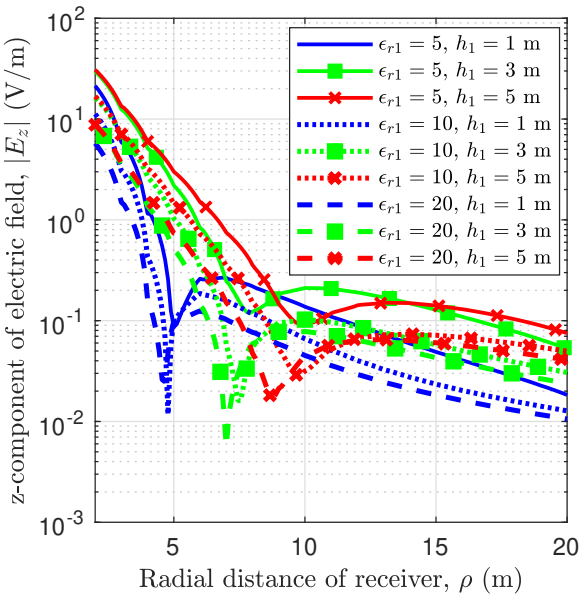

Fig. 5. Variation of $|E_z|$ with change of thickness and dielectric properties of the substrate, using an ideal dipole model

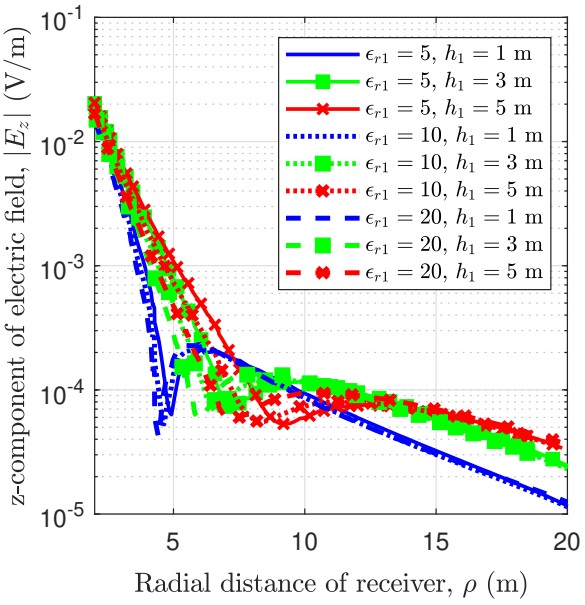

Fig. 6. Variation of $|E_z|$ with change of thickness and dielectric properties of the substrate, using a short dipole model

of the minima is the outcome of maximum impedance mismatch of the layered system with the source medium.

- With the increase of the dielectric constant with given thickness, the radial distance of the minimum position decreases. Again, after the minimum position is crossed, the magnitude rises and falls, and the fall is more for a lower thickness, which is expected.

The above arguments can also be inferred from the results of the ideal dipole simulation in COMSOL, as shown in Fig. 5. However, the minima locations in the graph appear to be

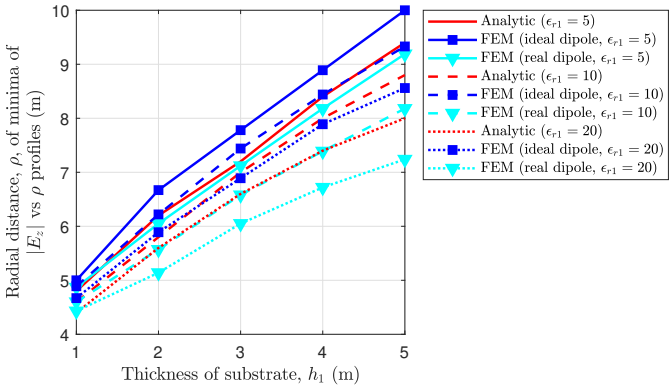

Fig. 7. Spatial distribution of the minima points observed in $|E_z|$ vs. ρ curves with increasing thickness of the dielectric substrate

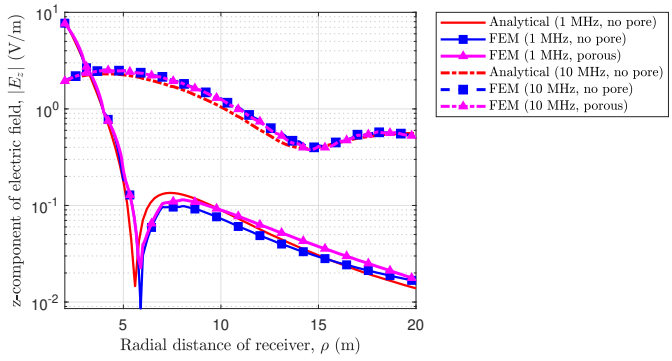

Fig. 8. Comparison of $|E_z|$ vs. ρ profiles for both homogeneous (no pores) and porous substrates, for an ideal dipole with operating frequencies of 1 MHz and 10 MHz. The chosen $\epsilon_{r1} = 20$, and the substrate thickness is 2 m.

slightly sparse compared to those obtained analytically. The other claims are similar to those obtained before. The E_z plots for a short practical dipole (Fig. 6) also agrees with the patterns, although in this case, the minima locations are more densely spaced in the graph compared to both the previous results.

The locations of the minima positions with increasing thickness are also observed for all three cases. Fig. 7 shows the radial distances of those minima positions vs. the varying thicknesses of the substrate. For all the three methods of measurement, it can be inferred that the shift of the minima locations is almost uniformly related with the increase of the substrate thickness. These results provide good information on the medium characteristics, and the LF measurements can be a promising method to determine the dimensions and dielectric constants of dielectric materials.

Furthermore, the FEM simulation results for the ideal and the real dipoles are in good agreement, and they are also reasonably close to those obtained by the analytical computation. Therefore, we can conclude that the FEM system can fairly accurately approximate the desired actual measurement environment.

Fig. 8 shows the $|E_z|$ vs ρ graphs for the complex geometry considering both pure and porous substrates. We see that the

inclusion of pores slightly changes the field profiles. This variation is not very much, as the minimum location appears to be almost unchanged with the inclusion of the pores. Even after increasing the frequency by a factor of 10, the effect of the pores appears to be negligible. This is not very surprising as the LF waves will have only minimal scattering from these inner impurities. Thus the effects of the properties and the dimensions of the substrate under consideration are still the major factors for shaping the outcomes of the LF measurements. This observation could not be performed using analytical techniques, and the advantage of the FEM model can be easily understood.

VI. Conclusion And Further Works

A method of developing a finite element simulation model to observe the response due to low frequency dipole radiation is presented. The behaviour of the LF electric fields in the presence of multilayered structures is investigated in the near-field region. Both analytical computations and FEM simulations were presented and the general conclusions obtained from both results are in good agreement. The electric field appears to show good changes with varying medium thickness and dielectric properties, both in terms of the minima locations and the magnitude profile. The effect of the inclusion of air pores inside the substrate is examined, and it appears that they do not significantly change the field pattern. While the field measurements suggest LF techniques as possible means of non-destructive measurement, the validated FEM model marks the possibility of investigating complex structures.

Acknowledgment

This work has been supported by the Office of Naval Research Global, London, UK [grant N62909-19-1-2013] as part of the NICOP project "Non-invasive measurement of sea ice thickness using low frequency EM waves".

References

[1] "Chapter vi - problems of radio," in *Partial Differential Equations in Physics*, ser. Pure and Applied Mathematics, A. Sommerfeld, Ed. Elsevier, 1949, vol. 1, pp. 236 – 296.

[2] J. R. Wait, *Electromagnetic Waves in Stratified Media*, 2nd ed. Oxford: Pergamon Press, 1970, ch. 1,2.

[3] F. N. Frenkiel and G. Temple, "Applied mathematics and mechanics: An international series of monographs," in *Waves in Layered Media*, ser. Applied Mathematics and Mechanics, L. Brekhovskikh, Ed. Elsevier, 1980, vol. 16.

[4] J. A. Kong, "Electromagnetic fields due to dipole antennas over stratified anisotropic media," *GEOPHYSICS*, vol. 37, no. 6, pp. 985–996, 1972.

[5] C.-M. Tang, "Electromagnetic fields due to dipole antennas embedded in stratified anisotropic media," *IEEE Transactions on Antennas and Propagation*, vol. 27, no. 5, pp. 665–670, Sep. 1979.

[6] Y. S. Kwon and J. J. H. Wang, "Computation of hertzian dipole radiation in stratified uniaxial anisotropic media," *Radio Science*, vol. 21, no. 06, pp. 891–902, 1986.

[7] L. Tsang, J. A. Kong, and G. Simmons, "Interference patterns of a horizontal electric dipole over layered dielectric media," *Journal of Geophysical Research (1896-1977)*, vol. 78, no. 17, pp. 3287–3300, 1973.

[8] J. R. Rossiter, G. A. LaTorraca, A. P. Annan, D. W. Strangway, and G. Simmons, "Radio Interferometry Depth Sounding: Part II - Experimental Results," *Geophysics*, vol. 38, no. 3, pp. 581–599, Jun. 1973.

[9] A. P. Annan, W. M. Waller, D. W. Strangway, J. Rossiter, J. D. Redman, and R. Watts, "The electromagnetic response of a low-loss, 2-layer, dielectric earth for horizontal electric dipole excitation," *Geophysics*, vol. 40, no. 2, pp. 285–298, Apr. 1975.

[10] W. C. Chew and J. A. Kong, "Electromagnetic field of a dipole on a two-layer Earth," *Geophysics*, vol. 46, no. 3, pp. 309–315, Mar. 1981.

[11] Le-Wei Li, Pang-Shyan Kooi, Mook-Seng Leong, and Tat-Soon Yee, "Electromagnetic dyadic green's function in spherically multilayered media," *IEEE Transactions on Microwave Theory and Techniques*, vol. 42, no. 12, pp. 2302–2310, 1994.

[12] A. Fallahi and B. Oswald, "On the computation of electromagnetic dyadic green's function in spherically multilayered media," *IEEE Transactions on Microwave Theory and Techniques*, vol. 59, no. 6, pp. 1433–1440, 2011.

[13] H. Moon, F. L. Teixeira, and B. Donderici, "Stable pseudoanalytical computation of electromagnetic fields from arbitrarily-oriented dipoles in cylindrically stratified media," *Journal of Computational Physics*, vol. 273, pp. 118–142, 2014.

[14] Y. Xu, W. Xue, Y. Li, L. Guo, and W. Shang, "Electromagnetic field analysis of an electric dipole antenna based on a surface integral equation in multilayered dissipative media," *Applied Sciences*, vol. 7, no. 8, p. 774, 2017.

[15] Y. Kiarashinejad, S. Abdollahramezani, M. Zandehshahvar, O. Hemmatyar, and A. Adibi, "Deep learning reveals underlying physics of light–matter interactions in nanophotonic devices," *Advanced Theory and Simulations*, vol. 2, no. 9, p. 1900088, Jul 2019.

[16] Y. Deng and J. G. Korvink, "Topology optimization for three-dimensional electromagnetic waves using an edge element-based finite-element method," *Proceedings of the Royal Society A*, vol. 472, no. 2189, 2016.

[17] K. Yao, R. Unni, and Y. Zheng, "Intelligent nanophotonics: Merging photonics and artificial intelligence at the nanoscale," *Nanophotonics*, vol. 8, no. 3, pp. 339–366, 2019.

[18] M. S. Islam, S. Shafi, M. I. Hasan, and M. A. Haque, "Low frequency near field interferometry for characterization of lossy dielectric and an investigation on sea ice," *IEEE Transactions on Geoscience and Remote Sensing (Early Access)*, pp. 1–11, 2020.

[19] W. C. Chew, *Waves and Fields in Inhomogeneous Media*. New York, NY: IEEE Press, 1995, ch. 1, 2.

[20] A. P. Annan, "Radio Interferometry Depth Sounding: Part I-Theoretical Discussion," *Geophysics*, vol. 38, no. 3, pp. 557–580, Jun. 1973.

[21] L. Tsang, R. Brown, J. A. Kong, and G. Simmons, "Numerical evaluation of electromagnetic fields due to dipole antennas in the presence of stratified media," *Journal of Geophysical Research (1896-1977)*, vol. 79, no. 14, pp. 2077–2080, 1974.

[22] J. Kong, L. Tsang, and G. Simmons, "Geophysical subsurface probing with radio-frequency interferometry," *IEEE Transactions on Antennas and Propagation*, vol. 22, no. 4, pp. 616–620, July 1974.

[23] J. J. H. Wang, "General method for the computation of radiation in stratified media," *IEE Proceedings H - Microwaves, Antennas and Propagation*, vol. 132, no. 1, pp. 58–62, February 1985.

[24] M. Siegel and R. W. P. King, "Electromagnetic fields in a dissipative half-space: A numerical approach," *Journal of Applied Physics*, vol. 41, no. 6, pp. 2415–2423, 1970.

[25] J. Hunziker, J. Thorbecke, and E. Slob, "The electromagnetic response in a layered vertical transverse isotropic medium: A new look at an old problem," *GEOPHYSICS*, vol. 80, no. 1, pp. F1–F18, 2015.

[26] M. Dautta, "Theoretical analysis of low frequency electromagnetic signal propagation in shallow seas," in *Proceedings of the 2016 International Conference on Communication and Information Systems*, 2016, pp. 25–29.

[27] ——, "Computation of electromagnetic field propagation characteristics of a dipole antenna submerged in sea-water," in *2016 International Conference on Wireless Communications, Signal Processing and Networking (WiSPNET)*, 2016, pp. 28–32.

[28] A. C. Polycarpou, "Introduction to the finite element method in electromagnetics," *Synthesis Lectures on Computational Electromagnetics*, vol. 1, no. 1, pp. 1–126, 2005.